JOURNAL OF GEOPHYSICAL RESEARCH, VOL. 105, NO. B12, PAGES 28,279–28,293, DECEMBER 10, 2000

New constraints on Antarctic plate motion and deformation from GPS data

Marie-Noëlle Bouin
Laboratoire de Recherche en Géodésie, Ecole Nationale des Sciences Géographiques
Marne la Vallée, France

Christophe Vigny
Centre National de la Recherche Scientifique, UMR 8538, Ecole Normale Supérieure, Paris, France

Abstract. Four years (1995-1998) of continuous Global Positioning System (GPS) data recorded by 11 permanent International GPS Service (IGS) stations in Antarctica and surrounding regions have been processed using an optimized method for regional geodetic networks. The 4-year time series has allowed us to extract nonlinear variations and constant horizontal velocities for all the stations. In December 1997 we have set up a permanent GPS station at Dumont d'Urville in Terre Adélie. The resulting data, along with those of the Scientific Committee on Antarctic Research (SCAR) campaigns (1995 and 1996) are included in our processing. A coseismic displacement (1 to 2 cm) is detected in the horizontal components of this station. We relate this to the March 25, 1998, M_w=8.1 Balleny Islands earthquake for which a dislocation model yields prediction in the right direction. For the six Antarctic stations the horizontal rates are very consistent with the rigid plate rotation, all the residual velocities are negligible (less than 2 mm/yr), except at O'Higgins in the head of the peninsula (7 mm/yr toward the continent). The position of the rotation pole (62.0°N, 146.7°W) and its rate (0.264°/Ma) are significantly different from the NNR-Nuvel-1A predictions for the Antarctic tectonic plate but are consistent with the Australian relative motion. The high horizontal residual in the peninsula area, where iceberg calving rates and ice shelf disintegration have recently increased, can be interpreted as the horizontal component of the elastic crustal response to the load variations.

1. Introduction

Present-day crustal motions occurring over the Antarctic continent can be produced by a variety of phenomena. First, variations of the mass of the Antarctic ice sheet since the Last Glacial Maximum (LGM) induce a viscoelastic response involving crustal and mantle mechanisms [*Farrell*, 1972]. Variations of the ice thickness in East Antarctica as deduced from relative sea level records covering long periods [*Nakada and Lambeck*, 1989; *Peltier*, 1994; *Tushingham and Peltier*, 1991] could reach values superior than 1000 m since the LGM (18,000 years). It has been shown by *James and Ivins* [1998] using the deglaciation model of *Denton et al.* [1991] than the resulting present-day vertical motions would reach 15 to 20 mm/yr near areas with the largest deglaciation rates, as the Ross Embayment but would remain inferior than 10 mm/yr on the East Antarctic coasts. The expected associated viscous horizontal motions consist in a slight divergence of 1 to 2 mm/yr over the whole continent, which could hardly be detected by current geodetic techniques. Moreover, uncertainties in the predicted rates of both vertical and horizontal components are important. The crustal behavior is influenced by many parameters such as the lithospheric thickness, mantle viscosity and deglaciation history that remain largely unknown.

In addition to these long-term ice mass changes, the Earth crust reacts more locally, elastically, to the present-day evolution of the Antarctic ice sheet. This behavior is controlled by accumulation, depending mainly on climatic parameters like air temperature and humidity and by the ablation rate of the ice shelves. The recent evolution of the West Antarctic Ice Sheet is still poorly constrained: the air temperatures are increasing on the Antarctic peninsula, resulting in higher accumulation and ablation rates. Different realistic ice sheet models predict either rapid melting and collapse of the ice shelves or increasing accumulation rates without any change in the ablation rates [*Bind-*

Paper number 2000JB900285.
0148-0227/00/2000JB900285$09.00

schadler, 1997; *Huybrechts*, 1994]. The predicted elastic uplifts around the Ross Ice Shelf and Filchner-Ronne Ice Shelf are slightly more than 10 mm/yr but reach only 6-7 mm/yr on the peninsula [*James and Ivins*, 1998]. This scenario does not include the recently observed acceleration of melting on the major West Antarctic Ice Shelves. As far as the horizontal motions are concerned, the present-day ice mass unloading could result in a slight convergence around the main discharge centers. This is in contrast with the divergence obtained in the viscous case, an elastic trend involving both lithosphere and underlying mantle.

At a larger scale it is necessary to take into account displacements of the tectonic plates. Estimating current values of relative plate motions and comparing them with those over several millions years [*DeMets et al.*, 1990] has been an important goal of Global Positioning System (GPS) analysis over the past 10 years [*Argus and Heflin*, 1995]. The GPS network includes several stations on the tectonic plates surrounding Antarctica, that is, Santiago (South America), Perth, Hobart and Auckland (Australia), and Chatham (Pacific), thus allowing us to deduce the relative motion of the Antarctic plate. All the plate boundaries around Antarctica as characterized by seismic or magnetic profiles are ridges. A less-known region is located between the southeast end of South America and the Antarctic peninsula, with the Scotia microplate [*Pelayo and Wiens*, 1989]. The precise locations and mechanisms of the different boundaries of this plate are not completely known yet. The south boundary along the Antarctic plate is usually defined as a set of ridges and transform faults called South Scotia Ridge. It extends from the Shackleton Fracture Zone and Bransfield Strait at its west end to the South Sandwich Trench at the east. From the intraplate tectonic point of view, the Antarctic plate is characterized by a stable and quiet behavior. The seismic activity remains located on the plate boundaries [*Okal*, 1981] (Figure 1). Therefore we expect very little intraplate deformation from tectonic origin.

Because of the expected low amplitude (less than 10 mm/yr) and time dependence of the motions we want to determine, we have chosen to analyze the Antarctic International GPS Service (IGS) data with a specific processing strategy. This strategy is adapted to the tectonics and postglacial rebound of Antarctica, as opposed to the processing strategy used by the global IGS analysis centers.

To sum up, the aim of this study is to assess the level of rigidity of the Antarctic plate, to compare its overall motion to the Nuvel-1A model, and to detect horizontal crustal deformations due to past and present-day deglaciation. First, we shall give a detailed presentation and discussion of our data analysis. Second, the quantitative results will be described. Readers interested mainly in this second part can proceed and read it directly.

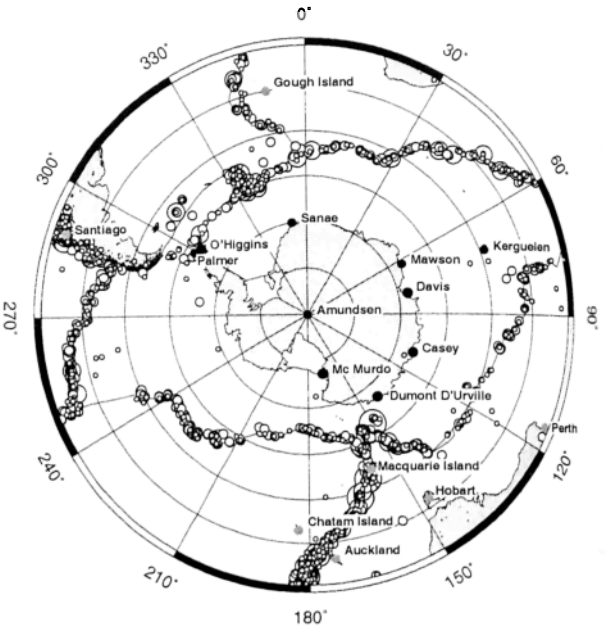

Figure 1. GPS stations used in this study. The tectonic plate boundaries are from the Nuvel-1 model [*DeMets et al.*, 1990] and the seismicity around the plate is after the centroid moment tensor catalog, earthquakes with $M_w \geq 4.5$ since 1977.

2. Data and Measurements

Our analysis includes all the permanent GPS stations available on the Antarctic plate since 1995. Most of these stations belong to the IGS global network and were installed in 1995, providing a quasi continuous data flow since then: Casey, Davis, McMurdo, and O'Higgins on the Antarctic continent itself and Kerguelen on the corresponding islands. Except for O'Higgins, all the stations are far away from the plate edge and should document the rigid plate rotation. In December 1997 a new IGS-like permanent station was installed at the French base of Dumont d'Urville, thanks to the financial and technical help of the Institut Français pour la Recherche et la Technologie Polaire (IFRTP). This GPS station is now running continuously. Because of technical problems in data transmission by International Maritime Satellite Organization, it is not possible to make them available within a reasonable time period. Nevertheless, this station should soon be included in the IGS network. The data from late 1997 till the end of 1998 have been processed in our analysis. The geodetic pillar chosen for this permanent station has been previously used during the 1995 and 1996 Scientific Committee on Antarctic Research (SCAR) campaigns. Data from these campaigns have also been included in our study. All analyzed sites are pictured Figure 1, while Figure 2 shows the data processed from 1995 to 1998.

There are four IGS stations on the Antarctic continent itself, providing data more or less continuously since 1995. All of them are located along the coasts.

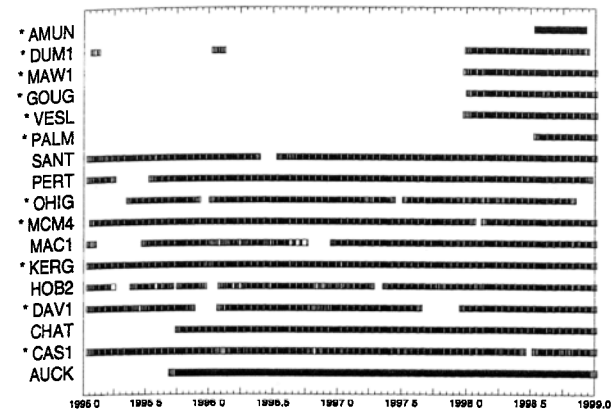

Figure 2. Available GPS data for all the sites used in this network, since the beginning of 1995, for the stations of Amundsen (AMUN), Auckland (AUCK), Casey (CAS1), Chatham Island (CHAT), Davis (DAV1), Dumont d'Urville (DUM1), Gough Island (GOUG), Hobart (HOB2), Kerguelen (KERG), Macquarie Island (MAC1), Mawson (MAW1), McMurdo (MCM4), O'Higgins (OHIG), Palmer (PALM), Perth (PERT), Santiago (SANT), and Sanae (VESL) (see Figure 1 for station identification). The stations within the Antarctic plate are marked by an asterisk.

In Antarctica, the main difficulty in installing permanent GPS stations for geodetic or geophysical purposes is to find ice-free areas, with bedrock outcrops. Direct access to the solid earth is prevented by the covering of the whole continent by an ice sheet up to 4500 m, except on a few areas, all located near the edge of the continent. This distribution is not ideally suited for the detection of vertical glacial rebound, as the most important postglacial movements are expected inland. Nevertheless, it provides a network geometry well adapted to measure plate tectonics velocities (with excellent spatial coverage) and to detect postglacial horizontal divergence. Data from four additional stations in Sanae (Veslekarvet), Amundsen, Mawson, and Palmer are available since 1998 (see Figure 2). The Amundsen permanent station is located at the South Pole base and built on the ice. Its motion is representative of the ice displacement only, but we have chosen to include it in our network, in order to reinforce the density of sites within the Antarctic continent.

To those stations located on the Antarctic continent itself, we can add the Kerguelen station, within the tectonic plate, far enough from the Australian-Antarctic ridge. As already mentioned, the only station in the vicinity of a plate boundary is O'Higgins, at the head of the peninsula, near the Bransfield Strait rift. For two reasons we have chosen to include some IGS stations outside the Antarctic plate in our network. The first reason is linked with the accuracy of our analysis. The addition of external stations increases the strength of the network. Second, we can use those additional stations to tie our network to a reference frame (International Terrestrial Reference Frame ITRF 97). This transformation will occur a posteriori relative to our GPS data analysis. Thus the sites used as reference stations must exhibit a stable behavior for the period of the analysis (1995-1998). More precisely, their ITRF 97 constant velocity must be representative of their motion during this period.

Among all the IGS sites surrounding Antarctica, we choose to use the six stations shown on Figure 1. Several stations were eliminated for different reasons, such as poor geodetic quality of the data, like in La Plata (Argentina), or stations which are too remote from the center of our network (South African stations), or installed too recently (Easter Island). Finally, some stations would be redundant with others in the same area (Australian stations). All the data included in our processing are presented in Figure 2.

3. Data Analysis

GPS data processing in Antarctica suffers from several specificities of this area of the world and benefits from a few of them. On the one hand, the size of the continent, the sparse network, and ionospheric activity considerably increase the difficulty of the task. On the other hand, the extreme dryness of the atmosphere and the unusually long satellite orbital arcs create more favorable conditions. All the data have been processed with the GPS scientific software GAMIT 9.1, developed at Massachusetts Institute of Technology (MIT). The current version of this software is an evolution of the first version described by *King and Bock* [1993]. GAMIT uses both carrier phase and pseudorange observables. The most precise information can be obtained by the carrier phase, but with ambiguities on the integer number of wavelengths. An unambiguous signal can be obtained by fixing these real numbers to the most probable integer value. The success of this step depends essentially on the quality of the signal and the length of the baselines. It is usually considered that this procedure is valid for baselines under 500 to 700 km. In Antarctica the ionospheric activity, which is especially high, introduces an additional noise which, under some circumstances, can produce cycle slips or prevent the signal recording itself. Using the ionosphere-free linear combination of two frequencies can help to remove the first-order of this ionospheric noise but results in an accentuation of the nondispersive noise. The lengths of the baselines of our network, between 1000 and more than 10,000 km, make ambiguity fixing impossible. All the solutions presented in this study leave the ambiguity nonfixed.

The considerable length of the baselines in the Antarctic network also reduces the quantity of double difference data (two satellites, two stations) which can be used for the GPS inversion. In this respect the introduction of Amundsen station increased the average

number of double differences from 120 to 136 and significantly contributed to the improvement of the repeatability after August 1998.

The dry component of the zenith tropospheric delay is implemented in the software by the *Saastamoinen* [1971] model. The wet component is estimated during the inversion, with zenith-delay adjustments every 3 hours, which apparently correspond to the best tradeoff between formal uncertainty and repeatability for two or more successive sessions [*Walpersdorf*, 1997]. However, the tropospheric activity above Antarctica is quite simple to model, the atmosphere being one of the driest in the world. Difficulties in evaluating the tropospheric zenith-delay parameters are generally due to large and rapid variations in the atmospheric rate of humidity, but such a rate remains more or less constant in the southernmost latitudes.

We have chosen the elevation cutoff angle as a tradeoff between the amount of data finally used in the processing and the relative accuracy. The geometry of the apparent orbits of the satellites over the South Pole, for positions at the Earth's surface below 60°S, is rather exceptional. Satellites avoid the zenith, remain for a long time at very low elevation, and make up for a bad zenithal distribution with a very good azimuthal layout. The elevation cutoff angle we used is 15°. This allows us to keep as much data as possible and to free ourselves from ionospheric and tropospheric noise coming from the lowest layers of the atmosphere.

Because of the length of the baselines in our network, the accuracy of our positioning is greatly influenced by the orbit accuracy, according to a direct proportional law. We have used the IGS precise combined orbits, which were available since the beginning of our analysis. A comparative study demonstrated that their precision is weaker over the Southern Hemisphere, because of the lack of IGS tracking stations. Nevertheless, the precision of these IGS orbits over the southernmost areas has been significantly improved from 1995 to 1998. All the data have been processed with fixed (not only constrained) IGS combined orbits and International Earth Rotation Service (IERS) B Earth Orientation Parameters. Since loose constraints have been applied to the positions, the reference frame after the GPS inversion is implicitly determined by one of the IGS orbits, ITRF 93 till the middle of 1996 and ITRF 94 after.

For our GPS inversion we have used a priori positions provided by the ITRF 96, when they exist. The weekly solutions currently used in IGS-type global processings introduce a smoothing effect in the time series. Since our intention is to obtain successive positions as disconnected as possible in time and independent of geodetic constraints, we have chosen to process only daily solutions (24-hour sessions).

4. Reference Frame

In our daily GPS processing, the a priori station positions are loosely constrained (100 m). Therefore the only constraint to a well-determined reference frame is implicitly provided by the fixed IGS orbits. This reference frame is absolute but arbitrarily defined and changes from day to day. In order to use the coordinates derived from our daily solutions for geophysical interpretation, we need to transform all our free solutions into a consistent and well-identified reference frame (ITRF 97) valid for the time span of our analysis.

4.1. Reference Stations

An optimal approach to express our free network in the ITRF is to select a subset of reference stations. Our daily positions on these stations and the ITRF 97 positions are constrained to be the same. For these stations at least, this implies that we assume a more or less linear behavior, as described by the reference frame solution itself (ITRF 97 is limited to linear displacements for all sites). Our reference stations, outside the Antarctic continent, have been chosen according to geographical or geodetic criteria. The first set of reference stations consists of three stations among the class A or B IGS stations, as described in the ITRF 96 and ITRF 97 quality assessment [*Altamimi*, 1998; *Altamimi et al.*, 1999]: Hobart (Australian plate), Kerguelen (Antarctic plate), and Santiago (South America). In Santiago we have to deal with a specific problem: although the IGS station belongs to the class A stations for position and velocity both in the ITRF 96 and ITRF 97 classifications, the geodetic quality of the data is poor (a manual cleaning is frequently required). In addition, this station is located on the South American tectonic plate, in the vicinity of the Nazca subduction zone. The motion of Santiago, largely influenced by the elastic coupling with the subducting plate, could significantly differ from its ITRF 97 linear behavior. Using this station as a reference station can thus influence the final results. Nevertheless, Santiago is the only station on the South American part of the network providing data of acceptable geodetic quality for such a long period. Hence its inclusion in the set of reference stations. The choice of the reference stations (Hobart, Kerguelen, and Santiago) provides a very good geographic coverage, with respect to the global geometry of our network (see Figure 1). In order to assess the sensibility of the results to the geometry of the reference stations, we have also tested an alternative set of reference stations with a weaker geometry. The comparison of the results shows negligible discrepancies. Therefore we have only used the first set, with the three stations above. We have tested two strategies to realize the reference frame with these reference stations. The first one is based on a Kalman filter, and the second one uses a seven-parameter transformation.

4.2. Kalman Filter Strategy and Baseline Adjustments

A solution is proposed by the GLOBK/GLRED software package developed as an interface with the

GAMIT software, combining global and regional GPS solutions using a Kalman filter [*Herring*, 1998]. It allows to combine individual sessions with station coordinates over several years of measurement, with or without stochastic parameters, resulting in station position and velocity estimations. In this study we assume that the behavior of the sites could be affected by nonlinear effects. We therefore seek to obtain time series of individual daily positions for each day of our GPS processing. Forcing time series positions to linear behaviors with high constraints could produce network distortions. To get round this problem, two different strategies are possible. First, we can estimate an averaged position and velocity over the entire time period (4 years), for every station of our network, and then run a backward solution to obtain individual positions for every day of GPS session. These individual sessions, for each day of the time series, are relatively uncorrelated if we introduce stochastic parameters in the backward solution for all the nonfiducial sites. When using this strategy for series longer than several years, the daily positions obtained on the reference stations (without stochastic parameters) are tightly constrained to the reference (ITRF) values, thus unsuited to our objective, that is, the study of tectonic implications.

The second way to proceed, using the same Kalman filter software, is to transform the free network into the ITRF values, estimating station positions only, with a daily session strategy. We obtain individual solutions for every 24-hour session, without explicit correlation between several successive sessions, even if it does not reflect the real geodetic behavior of the stations. The fiducial station positions will be closely constrained to the ITRF positions but with independent variations for each day. On the nonfiducial stations the results should be very similar to those of the previous method. The main difference is that this strategy produces usable results on the reference stations too, as their positions are not dependent any longer on ITRF values. In both cases nevertheless, using a Kalman filter leads to adjustments on the baselines, introducing an internal distortion in the network. These techniques will be especially sensitive not only to the choice of reference sites but also to data outage at the reference stations. For these reasons we have not used a Kalman filter method but a method of transformation, as described now.

4.3. Seven-Parameter Transformation and Coordinate Set Comparison

Another strategy is to transform sets of coordinates from the GPS analysis with a seven-parameter transformation. We have used the CATREF 1.1 software developed by *Altamimi* [1997] with the initial purpose of combining space geodetic solutions in positions or in both positions and velocities to produce ITRF solutions. Sets of coordinates from various spatial techniques are compared using a seven-parameter transformation, with a least squares adjustment. In our analysis we first determine transformation parameters by comparing day by day our free GPS solution with the ITRF corresponding solution. The seven-parameter transformation is then applied to our daily GPS free solutions, in order to realize a consistent reference frame for the entire duration of our time series. Unlike most studies transforming GPS coordinate sets into a reference frame, the different individual solutions are weighted using full variance-covariance matrices of the two sets in the least squares process. The station positions themselves are not exactly constrained, but the sites can be more or less weighted within the network for the seven-parameter estimation. We realize one transformation of the GPS free solution with the corresponding seven-parameter set for each individual daily session. Thus we obtain as many solutions as 24-hour sessions, which are as disconnected as possible from the ITRF constant velocities. We use this strategy in a day by day approach, estimating positions for every day of our series, without any estimation of velocities. This transformation strategy offers two noticeable advantages over the Kalman filter method. First, the global network geometry remains unchanged, as the seven-parameter transformation does not disturb the baselines. Their length is modified by the scale factor estimation, the global orientation and position of the network is changed by the rotation and translation parameters, but there are no other changes within the network. It also provides global transformation parameters, thus reflecting the time evolution of the transformed solution with respect to the initial reference frame. Second, the result is relatively independent from the choice of the fiducial stations. It minimizes the constraint effect brought by weighting on the comparison, which concerns all the points within the coordinate set.

For this study we have selected this reference frame realization strategy, using a daily seven-parameter transformation and Hobart, Kerguelen, and Santiago as reference stations. One could basically achieve a similar type of analysis using the GLOBK/GLORG software, as described in its latest release. From the daily coordinate sets transformed into the reference frame, we obtain new time series allowing us to extract linear velocities and short-term behavior for every site. These rates are estimated for each station, independently from the behaviors at other sites, by using simple linear regression.

4.4. Reference Frame: ITRF 97

Another relevant question is the choice of the reference frame itself, to transform our free solution. The IGS orbits were kept fixed all along our GPS processing and transformation into the reference frame. The implicit reference frame defined through the IGS orbits is ITRF 93 from 1995 to June 1996, ITRF 94 after this date. The a priori station positions used as input in our GPS processing are from ITRF 96. For consistency reasons the logical choice for our reference frame

should be ITRF 96. Nevertheless, the new realization ITRF 97 brings a significant improvement with respect to ITRF 96, leading to the recommendation of the use of ITRF 97 instead of ITRF 96 [*Altamimi et al.*, 1999], especially as far as the southern part of the IGS network is concerned. The IGS network has been locally densified, the time series used in the estimation of velocities are longer, the quality of the IGS orbits above the Southern Hemisphere has been improved. This yields a significant improvement of the positions and velocities of the IGS in and around Antarctica for the ITRF 97 solution. Therefore the final transformation of our free network (ENS 97) has been realized into the ITRF 97.

Although ITRF 96 and ITRF 97 are globally aligned in terms of datum definition, a nonzero transformation can occur between subsets of the two ITRF realizations. This is also true for the subset of core stations included by all the IGS analysis centers in their orbit processing, even if the transformation parameters are negligible. We have not applied any global transformation prior to the seven-parameter transformation used for the comparison of coordinate sets. To proceed rigorously, we should first define the appropriate transformation parameters from ITRF 96 to ITRF 97 for our subset of stations (this stage is done anyway by the CATREF seven-parameter transformation), then apply this transformation to our free solution. This additional transformation is thus included in the global transformation. To take into account the effect of changing the reference frame in the IGS orbit processing (ITRF 93 to ITRF 94, in June 1996), we apply an additional seven-parameter transformation to our free solution during all the periods before June 1996. The parameters are extracted from *Altamimi et al.* [1999] and correspond to the IGS core station transformation from ITRF 93 to ITRF 94 (13 common stations). All the time series are then implicitly expressed in the ITRF 96; after that we can transform them into the ITRF 97 using the CATREF 1.1 seven-parameter transformation. If we neglect this preliminary transformation on the period prior to June 1996, it will not change anything on the final transformed results, but the transformation parameter values on this period will be affected, since the additional implicit transformation will be absorbed. In this situation we observe a gap in the transformation parameter series when changing from ITRF 93 to ITRF 94 in the orbit processing.

4.5. Summary

Table 1 summarizes the processing strategy and parameters, including the GPS processing itself and the transformation of the free solution into a reference frame, as explained above in details. Most of the GPS data we have analyzed (except Dumont) are included in the global IGS network processing. Nevertheless, the utilization of a processing strategy thoroughly adapted to reveal tectonic implications leads to significantly improved results with respect to global solutions. As a matter of fact, our strategy for analyzing the GPS data and transforming our results into a consistent reference frame has been adapted to the geophysical objective of our study: detecting internal deformations without applying unconsidered external a priori constraints. Moreover, the careful reprocessing of a subset of stations makes an improved cleaning of the data possible. This is obtained both by adapting automatic edition parameters to Antarctic conditions and by the manual super-

Table 1. Data Analysis Summary

Parameter	Description
	GPS Processing
GPS software	GAMIT 9.1
Sessions	24 hours
Orbits	IGS precise orbits, fixed
Earth orientation parameters	IERS bulletin B
Elevation angle cutoff	15°
Phase ambiguities	Free (not resolved)
Tropospheric dry delay model	Saastamoinen
Tropospheric wet delay	Estimated every 3 hours
A priori station positions	ITRF 96
Station position constraints	Free network approach
	Transformation Into a Reference Frame
Transformation	Daily
Reference frame	ITRF 97
Strategy	Seven-parameter transformation, full variance/covariance matrix
Software	CATREF 1.1
Reference stations	3 (Hobart, Kerguelen, and Santiago)
Velocity estimation	Linear fit on the transformed daily time series

vision and the edition of peculiar data sets. This reprocessing leads to reincorporation of a significant amount of data (otherwise rejected by automatic procedures). Therefore, although it may come from the same original records, our final data set is cleaner and contains more information than the global sets of solutions. A considerable increase of the strength and precision of our solution is finally obtained.

5. Results

The 4-year-long time series we have obtained (ENS 97) allows us to extract various types of periodic or short-term variations. As an example, Figure 3 depicts the three components (north, east, and ellipsoidal height) for the position of the Antarctic station of Casey (variations are in meters). From these daily positions we can evaluate with an extremely good accuracy a linear trend for the two horizontal components. For clarity the formal uncertainties (between 0.3 and 1.2 cm) are not represented. At the beginning of 1997 we observe an abrupt variation of the ellipsoidal height reaching approximately 8 cm, followed by the rapid return to the mean value in November 1997. This probably reflects the damage of the radome covering the GPS permanent antenna, which occurred during spring 1997. This radome has been replaced by a new one by the end of the year 1997, as suggested by the time series variations. The date for the change of this radome, as given by IGS log for Casey, is approximately 1 month later than the jump observed in the time series. A possible scenario, according to B. Twilley (personal communication, 2000) is the following: the hole in the radome, covering one third of its surface, let the snow accumulate over the antenna itself and produced the first change in the vertical component; in November this snow all melted out, and the height measured returned to its mean value before the change of the radome (December 9, 1997). This point underlines the necessity of working with continuous and dense data in order to measure very tiny and slow displacements, especially on the height component, and the importance of getting reliable and precise information about the status of antennas and receivers. This information, which is easily obtained inside populated areas, is of critical importance for remote and unaccessible sites like Antarctica. The examination of those time series shows a high scatter of the daily positions during 1995 (due to the poor relative quality of the IGS orbits over the Southern Hemisphere), which reduces progressively until 1997 (improvement of the IGS orbits). In 1998 the introduction of new permanent GPS stations in the Antarctic network improves the constraint on the continental domain and reduces again the scatter of positions. Linear trends were fitted, in the least squares sense, to the time series on the whole period 1995-1998.

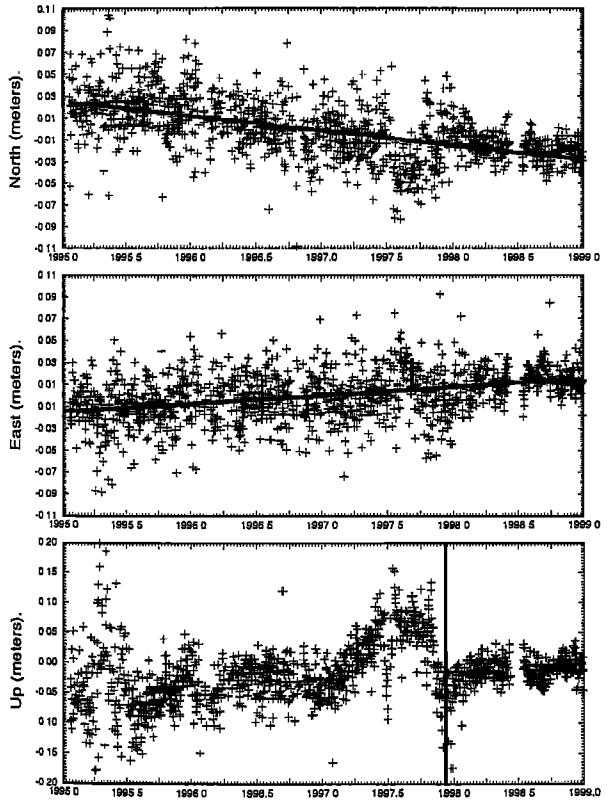

Figure 3. Time series for the three components in Casey, from the beginning of 1995 till the end of 1998: (top, middle) horizontal components and (bottom) vertical variations. The variations of the daily positions tied to the ITRF 97 are given in meters. The vertical component shows the 8-cm excursion corresponding to the damage of the radome covering the GPS antenna. The vertical line indicates the date of the change of the radome.

5.1. Dumont d'Urville

At Dumont the velocities have been extracted from time series including the SCAR 1995 and 1996 campaign data (10 days in January 1995 and 20 days in January and February 1996; see Figure 4). Close analysis of the recent continuous time series (Figure 5) shows an anomalous motion around March 25, 1998. At this date the largest intraplate earthquake ever recorded occurred in the vicinity. The hypocenter has been located near the Balleny Islands (62.9°S, 149.5°E) off the George V Land coast. This M_w=8.1 event occurred to the West of the Antarctic-Australian-Pacific triple junction (250 km). It seems to have ruptured a fault, or a series of strike-slip fault segments, nearly 300 km long, with a quasi-vertical slip [*Nettles et al.*, 1998]. The strike of the faults, according to the aftershocks, is 287°, nearly perpendicular to the north-south trending fossil fracture zones, forming the most visible bathymetric features of this region. Although this earthquake is well studied using teleseismic data and aftershock locations, the lack of recording stations and of surface displacement data in the area introduces a 25 km uncertainty in the location of the fault rupture. Its depth should not exceed 30 km

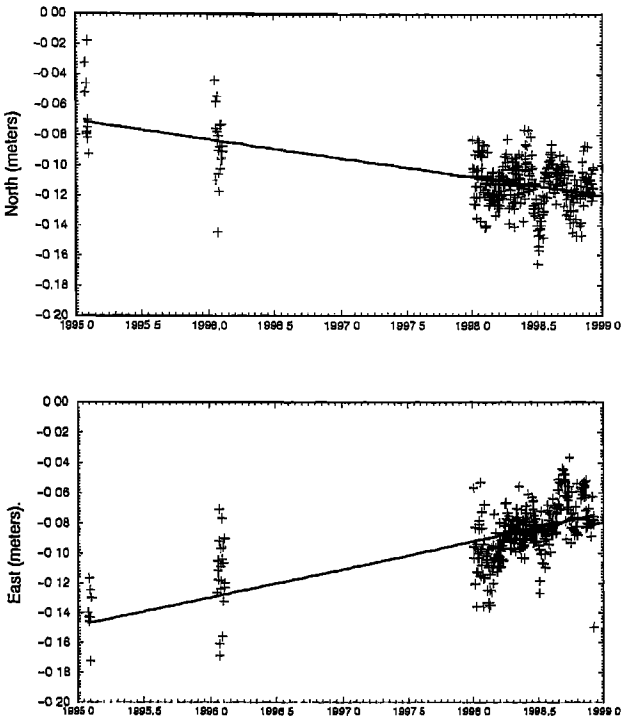

Figure 4. Time series for the horizontal components in Dumont (variations in meters) from the beginning of 1995 till the end of 1998. The SCAR campaign data (January 1995 and January 1996) are included. The trends correspond to uncorrected velocities (see text).

but is not yet known with better accuracy. The static Coulomb failure stress change related to this event has been calculated by *Toda and Stein* [2000] using four rough models for the dislocation mechanisms. The nearest GPS station to the assumed epicenter of this event is the new permanent station of Dumont, located at 66.4°S, 140.0°E, approximately 600 km from the mainshock. The induced coseismic displacement at the site of Dumont has been computed using an elastic dislocation code based on the equations of *Okada* [1992], which is very consistent with the *McGuire et al.* [1998] model. The predicted coseismic displacement according to this model is 22.4 mm along the east component, 19.4 mm along the north component, with large uncertainties due to errors on the main rupture location, the seismic moment, and to the plane approximation inherent in all dislocation codes (see Figure 6). We attempted to extract the observed coseismic displacement from the GPS time series in Dumont, for both north and east components, and compare them to the predicted values. The date of March 25, 1998, is indicated on the time series for the horizontal components in Dumont (Figure 5). We have evaluated linear trends to obtain horizontal velocities for the period before the seismic event (from the beginning of 1995 till March 25, 1998, thus including the 1995 and 1996 SCAR data) and for the period following the event (from March 25, 1998, till the end of the year 1998). The observed velocities before the event are 12 mm/yr and -15 mm/yr for east and north components, respectively. For the period after the event, we obtain 26 mm/yr and -10 mm/yr for east and north components, respectively. The uncertainty on the rate after the earthquake is larger than the uncertainty before, as the time series is shorter. The step between the two linear trends gives us the value of the instantaneous coseismic displacement as measured by GPS. It reaches 13 mm on the east component and 4 mm on the north component, less than the predicted values from the dislocation models estimation (22.4 mm and 19.4 mm) but quite compatible in orientation. Therefore the fact that the measurements exhibit, despite rough assumptions and high uncertainties, a displacement in the same direction and with a comparable amplitude than the predicted displacement clearly indicates that this is not an artifact. These horizontal coseismic displacements have been removed from the horizontal linear velocities at Dumont. The corrected velocities for the whole period are 15 mm/yr on the east component and -13 mm/yr on the north component. This matches well with the linear rates for the period before the earthquake (12 mm/yr and -15 mm/yr).

5.2. Global Plate Motion

The horizontal velocities, for all the stations in our network (including the stations outside the Antarctic

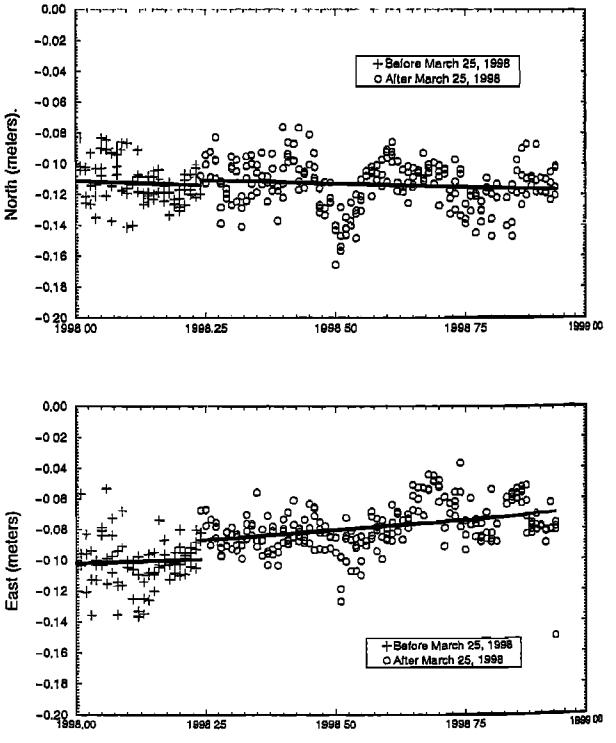

Figure 5. Time series for the horizontal components in Dumont. The date of March 25, 1998, is clearly indicated, and the trends are deduced before and after the event. The SCAR campaign data (January 1995 and January 1996), although used for computing the preseismic velocities, are not shown here.

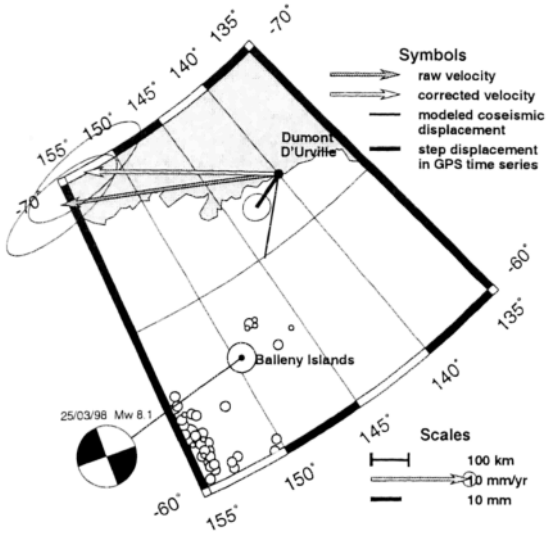

Figure 6. Location of the March 25, 1998, 8.1 event near Balleny Islands, with focal mechanism. At Dumont the uncorrected velocity (shaded arrow) and corrected velocity (open arrow) are indicated, as well as the coseismic displacements (solid segments) deduced from the GPS time series and predicted by the dislocation model.

plate), are summarized in Table 2. The uncertainties given in this table are of two different types. The 95% confidence limits on the velocities correspond to white noise assumption on the station behavior and are clearly underestimated. We also indicate the uncertainties corresponding to the differences on the horizontal rates obtained by using different ways of tying our free network to a reference system, as described previously. They are larger than the formal uncertainties but reflect the precision we can expect from our analysis in a more realistic way. Figure 7 shows these horizontal velocities for all the stations of the network, with related error ellipses. Our solution is compared with the rates predicted by the NNR-Nuvel-1A model [*Argus and Gordon*, 1991] and the ITRF 97 velocities when existing. The ITRF 97 solution includes IGS solutions, but also satellite laser ranging, doppler orbitography and radiopositioning integrated by satellite (DORIS), and very long baseline interferometry data.

For all the stations outside the Antarctic tectonic plate, the agreement between our solution and the ITRF 97 velocities is excellent. This confirms, from the geodetic point of view, the very good quality of our solution. For all the stations inside the Antarctic plate, we observe significant discrepancies between our solution and the ITRF 97. The most important difference is obtained in Dumont. We must point out that the ITRF 97 solution in Dumont is derived from DORIS data only partly because the new permanent GPS station on the French base is not yet included in the IGS network, as the data are not available in real time. In this situation, with collocation by two different techniques (GPS and DORIS), we infer a significant disagreement between them. We think that the GPS-determined velocity is probably more reliable since it is more consistent with other GPS velocities on the continent and with the plate rotation discussed below.

In Kerguelen, another place with GPS/DORIS collocation, the evolution of the velocities shows a convergence of the ITRF solutions toward our solution. More precisely, the ITRF 96 velocity on Kerguelen was very different from the NNR-Nuvel-1A (NNR-A) prediction. The ITRF 97 velocities come closer to both NNR-A and our solution, which itself remains untouched by the shift from ITRF 96 to ITRF 97. Still, both our and ITRF 97 solutions slightly and consistently differ from NNR-A.

The systematic disagreement between the two geodetic solutions (ENS 97 and ITRF 97) on all the Antarctic sites is related here to the misuse of the data from this part of the network in the global IGS processings conducted by most IGS analysis centers. Because the IGS global analysis includes stations covering the entire world, with a greater density of sites in the Northern Hemisphere (mainly North America and Europe), an obvious tendency is to neglect the data of poorer geodetic quality from the southern part of the network. One of the interests of our study is precisely to focus on the only stations on and around Antarctica. It leads, with an appropriate processing method, to results of increased quality on these stations.

On the stations outside the Antarctic plate, the agreement with the NNR-Nuvel-1A predictions is rather good. The sites showing discrepancies are located near the plate boundaries and are affected by local tectonic

Table 2. Station Velocities V, 95% Confidence Limits assuming White Noise (σ) and Standard Deviations Corresponding to Realistic Estimate of Confidence Limits (Δ), ENS 97

	East			North		
Station	V^a	σ	Δ	V	σ	Δ
AUCK	6	±1	± 6	32	±1	± 7
CAS1	8	±1	± 6	-13	±1	± 5
CHAT	-40	±1	± 5	27	±1	± 6
DAV1	2	±1	± 6	-10	±1	± 4
DUM1[b]	19	±2	±10	-12	±2	± 3
DUM1[c]	15	±2	±10	-13	±2	± 3
HOB2	15	±1	± 4	50	±1	± 5
KERG	8	±1	±10	-10	±1	± 3
MAC1	-9	±1	± 6	25	±1	± 4
MCM4	14	±1	± 8	-11	±1	± 5
OHIG	13	±1	± 5	5	±2	±20
PERT	40	±1	± 2	49	±1	± 2
SANT	20	±1	± 7	14	±2	±20

[a] Units are in mm/yr
[b] Noncorrected velocity.
[c] Coseismic displacement removed.

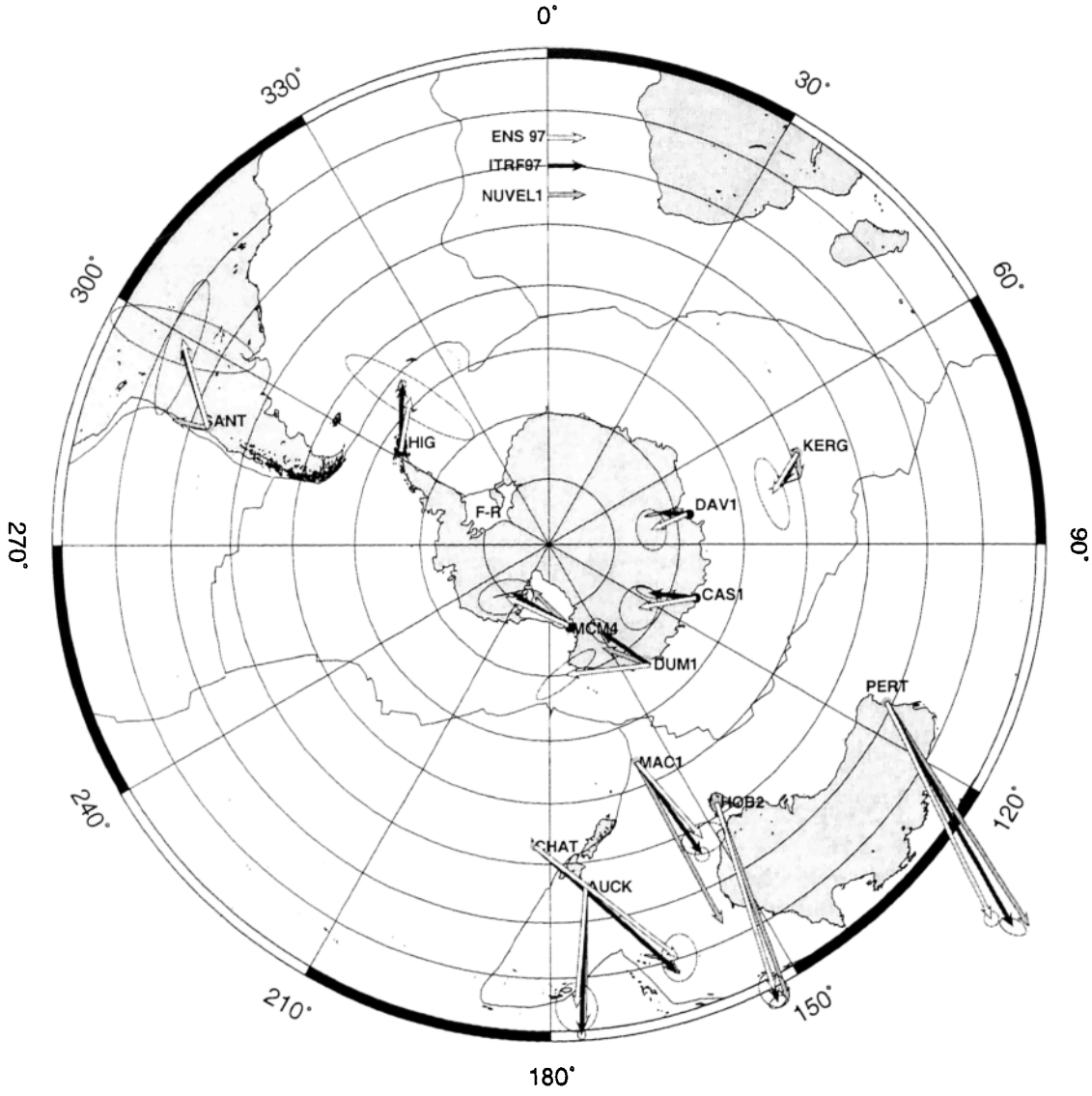

Figure 7. Velocities for our solution (open arrows), in comparison to the ITRF 97 velocities (solid arrows) [*Boucher et al.*, 1999] and the NNR-Nuvel-1A (shaded arrows) velocities [*Argus and Gordon*, 1991]. The scale of 10 mm/yr is given at the top of the figure. The error ellipses represent the differences between all the solutions obtained when transforming our network into the ITRF 97 with different methods. The two main ice shelves of Filchner-Ronne (F-R) and Ross are indicated in light grey.

motions, like in Santiago and Macquarie Islands. The horizontal velocity in Macquarie Islands is very consistent between the two geodetic solutions but slightly differs in amplitude and orientation from the NNR-A model predictions. This can be related to the vicinity of the Australian-Pacific plate boundary. The motion of Santiago in the NNR-A model is assumed to reflect only the South American plate motion, while the elastic coupling with the nearby Nazca subduction zone is obvious in both geodetic solutions, with an additional component of more than 20 mm/yr parallel to the subduction direction.

For all the stations located in the stable Antarctic plate interior, the discrepancies with the NNR-A predictions are significant. For example, our estimate in Kerguelen disagrees by more than 45° in orientation with the NNR-A velocity. All our horizontal rates on the stable Antarctic plate, even though they are significantly different from the NNR-A predictions, happen to strongly point to a rigid plate rotation. We have evaluated a rotation plate motion, expressed as usual in terms of best pole of rotation and angular speed corresponding to the stations velocities by the way of the very simple relation written as

$$v = \omega \times r \tag{1}$$

where v is the velocity of the site, ω is the angular velocity of the Antarctic plate, and r is the position of the

Table 3. Best Rotation for the Antarctic Plate (rotation velocity in degrees per millions of years and position of the pole), in Comparison With the NNR-Nuvel-1A Predictions[a]

	Angular Velocity deg/Myr	Latitude °N	Longitude °W
ENS 97	0.264	62.0	146.7
NNR-Nuvel-1A	0.24	63.0	115.9

[a]Rotation velocity in degrees per millions of years and position of the pole

site inside the plate. All the velocities v, which could be three-dimensional, are here explicitly horizontal (two components per station). In what follows, all the plate velocities are expressed in terms of position of the pole of rotation (latitude, longitude) and angular velocity.

The rotation motion is estimated using the stations of Casey, Davis, Dumont, Kerguelen, McMurdo and O'Higgins, all located in the interior of the Antarctic plate. The time series obtained from the data of the geodetic pillar in Dumont is covering a time period of almost 4 years, as for the other stations running continuously. We have thus used the Dumont velocity together with the other Antarctic rates in our estimation. To confirm that its use will not modify the global plate motion, we have compared both solutions obtained with or without including this station. The difference between both solutions is less than 0.01°/Ma in the angular speed, and less than 0.3° in latitude and longitude for the best pole position. Table 3 lists our pole position and angular velocity along with the NNR-A predictions.

Figure 8 depicts the residual velocities, obtained for each site: differences between observed velocities and those corresponding to the rigid plate rotation. They are all negligible (less than 2 mm/yr, see Figure 8), except for the O'Higgins station. Such a result cannot be obtained from the ITRF 97, for example, since the residual velocities remain significant and inconsistent for several stations. This confirms the good geodetic quality of our results, together with the rigid behavior of the Antarctic plate at this level of precision. It also confirms the reality of the coseismic step in Dumont time series, since the residual at this station reaches a value close to zero only when this correction is applied. Interestingly enough, the position of our pole of rotation (see Table 3) is significantly different from the NNR-A prediction for the Antarctic plate. This point is discussed in the next section.

At O'Higgins, we observe a significant residual velocity of more than 7 mm/yr, directed toward the interior of the continent. The station is located at the head of the peninsula, in an ice-shelf collapse area. The data about the present-day ablation rate of the ice sheet in this part of West Antarctica are still lacking, but this rate is suspected to be high. It is likely that the thinning rate, hence the glacial vertical and horizontal motions, are still underestimated by the current models. This horizontal residual velocity of 7 mm/yr could be interpreted here as the horizontal component of an elastic rebound local motion (for the Antarctic peninsula) directed toward the center of maximum ice load changes (foot of the peninsula or Filchner-Ronne Ice Shelf).

6. Discussion

Except at the O'Higgins station, which is affected by glacial rebound or local tectonics, all our horizontal velocities are very consistent with a rigid plate rotation but show a significant and systematic discrepancy with

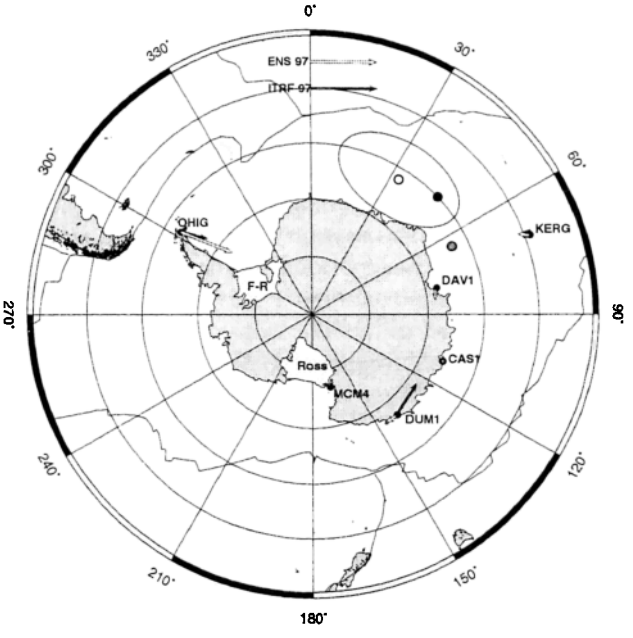

Figure 8. Residual velocities for the Antarctic stations after removal of the best rigid rotation estimation (open arrows) in comparison with the ITRF 97 residual velocities (solid arrows) for the same sites. The scale of 10 mm/yr is given at the top of the figure. The positions for the respective best pole positions are indicated by the corresponding open and solid points. The shaded point indicates the position of the NNR-Nuvel-1A rotation pole. The two main ice shelves of Filchner-Ronne (F-R) and Ross are indicated by the light grey areas.

Table 4. Absolute Rotation Pole for the Australian Plate From Different Solutions

	Angular Velocity deg/Myr	Latitude °N	Longitude °E
M.B. Heflin (JPL website)	0.64	34.1	43.5
ENS 97	0.55	33.7	40.2
Larson et al. [1997]	0.61	31.4	40.7
NNR-Nuvel-1A	0.65	33.8	33.2

the NNR-A predictions, suggesting a further search for additional confirmations.

6.1. Plate Rotation

The Nuvel-1 model for the Antarctic plate is mainly constrained by the relative motion with the Australian plate. More precisely, the data concerning the Australian-Antarctic ridge provide a better geometric coverage with respect to the Euler pole for the relative motion on this boundary, than, for example, the data from the Antarctic-South American boundary [*DeMets et al.*, 1990]. On the Antarctic-African plate boundary too, the Nuvel-1 motion is deduced from closely spaced data, providing only a weak constraint. The less-known relative motions concern the Pacific plate, where data are especially sparse, and the Scotia plate, which is not taken into account in Nuvel-1. All the motions deduced by Nuvel-1 from the data on the boundaries with the African and South American plate yield systematically poor fits, with rates 1-3 mm/yr slower than observed [*DeMets et al.*, 1990]. This effect is even enhanced in Nuvel-1A [*DeMets et al.*, 1994]. Therefore it makes more sense to compare relative motions for the Antarctic-Australian boundary derived from our results to the same relative motions predicted by Nuvel-1A, than to compare absolute plate motions. As pointed out by *Larson et al.* [1997], relative motions are less sensitive than absolute plate motions to reference frame errors in the geodetic results, or the no-net-torque assumption used in NNR-A. We can compare relative velocities for the Antarctic-Australian plates with the relative motion predicted by Nuvel-1A. Our results on Australia (stable interior) include only three stations (Auckland, Hobart and Perth), so we cannot expect to deduce a precise pole for this plate. Another recent result from spatial geodetic techniques concerning the Australian plate is provided by M.B. Heflin (World Wide Web site of the Jet Propulsion Laboratory, *http://sideshow.jpl.nasa.gov/mbh/series.html*), (hereinafter referred to as JPL website) for the IGS global solution of the Jet Propulsion Laboratory (JPL). This solution, one among many IGS analyses, has the advantage to include recent data, the time series covering all the 1998 data. Using the method previously exposed, horizontal velocities on the stations of Auckland, Canberra, Cocos, Hobart, Perth, Tidbinbilla and Yaragadee supply an angular velocity and pole position with an extremely good accuracy (see Table 4). The position of the pole and the angular speed obtained after M.B. Heflin (JPL website) are also significantly different from the NNR-A predictions for the Australian plate but relatively close to our results for the same plate (less than 3° on the east and north component of the pole position, estimated from three stations only). We can thus estimate a relative motion for the two Australian and Antarctic plates, using our results on the Antarctic plate and M.B. Heflin (JPL website) velocities on the Australian plate. The relative angular motion is obtained very simply by differencing the absolute angular velocities of the two independent plates. We have compared our relative velocity (pole position and angular relative speed) with the geodetic results obtained by *Larson et al.* [1997] for the same relative motion and the Nuvel-1A predictions [*DeMets et al.*, 1994] (see Table 5). *Larson et al.* [1997] used GPS data during the time span 1991-1996 to estimate the absolute and relative global plate velocities. Only the sites providing more than 2 years of data were included in the analysis: the Antarctic plate motion is determined from only the two stations of McMurdo and O'Higgins, and should be taken with great care. The Australian absolute motion is derived with a better accuracy using the 6 sites

Table 5. Relative Angular Motions for the Australian/Antarctic Plates From Different Solutions

	Angular Velocity deg/Myr	Latitude °N	Longitude °E
M.B. Heflin (JPL website)/ENS 97	0.66	10.92	41.6
Larson et al. [1997]	0.65	9.8	43.2
Nuvel-1A	0.65	13.2	38.2

of Canberra, Hobart, Perth, Townsville and Yaragadee (see Table 4). This Australian GPS motion is close to the recent (M.B. Heflin, JPL website) solution, as the pole position discrepancy is less than 3° in both latitude and longitude and 0.03°/Ma in angular speed. Our relative Antarctic/Australian angular velocity (Table 5) is very close to the *Larson et al.* [1997] relative motion and to the Nuvel-1A estimate (0.01°/Ma difference on the angular speed and less than 3.5° on the position of the pole, both components). The two GPS solutions (ENS 97/Heflin and Larson et al.) are thus very consistent with each other and show a good coherence with the Nuvel-1A prediction too. Since this Nuvel-1A relative motion provides the main constraint on the absolute motion of the Antarctic plate itself, our result, associated with the M.B. Heflin (JPL website) solution, agrees finally very well with the Nuvel-1A predicted relative motion for the Australian and Antarctic plates.

We can turn back to our Antarctic angular velocity, which is significantly greater than the absolute NNR-A prediction. For Nuvel-1, *DeMets et al.* [1990] mention a systematic underestimation of observed opening rates between Antarctica and the South American, African, and Nazca plates. This misfit, which increases in the Nuvel-1A correction [*DeMets et al.*, 1994], is attributed to nonclosure within the three-plate circuit (Antarctica, South America, and Africa). Therefore we consider that it is not very surprising that a direct determination of the Antarctic rotation pole, from space geodetic techniques, significantly differs from the Antarctic pole in Nuvel-1A.

6.2. Glacial Elastic Rebound

On the O'Higgins station, at the head of the peninsula, our important horizontal residual velocity (7 mm/yr toward the interior of the continent) could reflect the horizontal component of an elastic glacial rebound displacement. This velocity might be consistent with an elastic convergence around the discharge center located in the head of the peninsula. Opposite to the horizontal part of the viscoelastic long-term glacial rebound which consists in a slight divergence, the elastic instantaneous response to a removal of the load results in a convergence around the main discharge center. In addition, the associated vertical velocity, although less accurately determined, indicates a significant uplift (10 to 15 mm/yr for the elastic part) [*Bouin*, 1999], reflecting the recent increase of the ice melting on the peninsula and, partly, on the West Antarctic Ice Sheet. This vertical velocity of 10 to 15 mm/yr would correspond to a steady ablation rate of the ground ice sheet, of 60 to 75 cm/yr, according to the simple loading/unloading model proposed by *James and Ivins* [1998], using the *Farrell* [1972] values. These values are higher than assumed in most of the commonly used ice sheet models [*Bentley and Giovinetto*, 1991; *Giovinetto and Bentley*, 1985; *Verbitsky and Saltzman*, 1995] but still comparable with the maximal melt rates considered by one of the models of *Jacobs et al.* [1992], reaching 689 mm/yr locally. This model is the only scenario taking into account glacial thinning over West Antarctica in a more or less realistic way. It should be noted that all these rates are mean values and generally neglect the acceleration of iceberg calving and ice shelf collapse, as observed along the peninsula coasts since the beginning of the 1990s [*Rott et al.*, 1996; *Skvarca*, 1994]. If we assume that such events affect not only the marine ice shelves, but also the ground ice sheet, the present-day ablation is largely higher than assumed in the ice sheet models. On restricted areas of grounded ice sheet, leveling surveys coupled with radar measurements have shown a steady ablation rate of 32 cm/yr during 20 years on the Rothera ramp [*Smith et al.*, 1998]. The present-day ice behavior on the peninsula, which is still unknown for a large part, is probably consistent with an important increase of the ablation rates. This could be confirmed by leveling studies on the Japanese base of Syowa showing a regular uplift (10 mm/yr) during the last 20 years [*Kamimuna*, 1998]. Another explanation for O'Higgins motion might be local tectonics related with the Bransfield Strait and the Scotia microplate but without any evidence from, for example, *Salbach and Niemeier* [1998] and *Dietrich* [1998].

7. Conclusion

In this paper we have presented the results for the analysis of a 4-year series of GPS data in Antarctica. The data from the newly installed (end of 1997) Dumont GPS permanent station and from the previous SCAR campaigns (same point, 1995 and 1996) were included in our processing. All the other stations are IGS stations. Most of the data we used were already included in the global IGS analysis. Our analytical method has been carefully adapted to our geophysical goal. This effort aims specifically at tying our free network to an international reference frame without polluting local displacements by inappropriate constraints. The horizontal velocities extracted from our time series show very good accuracy. We have also paid a great attention to the data, cleaning and editing them carefully, which is an impossible task for global IGS processing, but still manageable for a subset of chosen stations. We are able to compare our velocities with those of other geodetic analyses (namely, the multitechnique ITRF 97) and with the absolute plate motion model NNR-Nuvel-1A. For all the non-Antarctic sites the agreement between our solution and the ITRF 97 results is excellent, except for a few sites, located near the plate boundaries (Santiago and Macquarie Islands). On the Antarctic plate itself, we point out a significant and systematic discrepancy at all the stations. Our rates are very consistent with a rigid plate motion for Antarctica, but significantly different from the NNR-Nuvel-1A predictions. Our pole is located at 62.0°N, 146.7°W, with an angular speed of 0.264°/Ma, faster than the NNR-A predicted rotation. We have compared the relative motion deduced

from our angular velocity for Antarctica and from the newly proposed motion of M.B. Heflin (JPL website) for the Australian plate, with the Nuvel-1A relative motion as well as that obtained by *Larson et al.* [1997]. The agreement being extremely good, we can propose a new plate motion for Antarctica, in agreement with the M.B. Heflin (JPL website) new solution for Australia. All the residual velocities are less than 2 mm/yr, except at O'Higgins, on the peninsula. This residual velocity is interpreted here as the horizontal component (shrinking) of the elastic rebound corresponding to the present-day acceleration of melting on the Antarctic peninsula and accompanied by a rapid uplift of this station. At Dumont the accuracy of our time series allows us to detect a coseismic displacement, related to the March 25, 1998, M_w=8.1 earthquake, in good agreement with the dislocation model predictions.

Acknowledgments. We are grateful to the IFRTP for financial support, installing and maintaining the Dumont permanent GPS station. We would like to thank Hugo Perfettini for processing the coseismic motion prediction in Dumont. We especially thank Zuheir Altamimi who provided the CATREF software and for his helpful contributions concerning the reference frame and transformation part of this work. Michael Heflin, Don Argus, and an anonymous editor provided many useful suggestions for improvement of the manuscript.

References

Altamimi, Z., Analyse d'un logiciel de combinaison de positions et vitesses tridimensionnelles, *MM 17*, Publ. LAREG sér. mem., Lab. de Rech. en Géod., Ecole Nat. des Sci. Géogr., Marne la Vallée, France, 1997.

Altamimi, Z., IGS reference stations classification based on ITRF96 residual analysis, in *IGS 1998 Analysis Center Workshop Proceedings*, edited by J. Dow, J. Kouba, and T. Springer, pp. 177–182, ESA/ESOC, Darmstadt, 1998.

Altamimi, Z., C. Boucher, and P. Sillard, ITRF97 and quality analysis of IGS reference stations, in *IGS 1999 Analysis Center Workshop Proceedings*, edited by Y. Bock and T. Springer, SIO, La Jolla, 1999.

Argus, D., and R. G. Gordon, No-net rotation model of current plate velocities incorporating plate motion model NUVEL-1, *Geophys. Res. Lett.*, *18*, 2039–2042, 1991.

Argus, D. F., and M. B. Heflin, Plate motion and crustal deformation estimated with geodetic data from the Global Positioning System, *Geophys. Res. Lett.*, *22*, 1973–1976, 1995.

Bentley, C., and M. Giovinetto, Mass balance of the Antarctic ice sheet and sea level change, in *Polar Regions and Climate Change, Proceedings of Symposium*, edited by G. Weller, C. Wilson, and B. Severin, pp. 481–488, Univ. of Alaska Press, Fairbanks, 1991.

Bindschadler, R. A., West Antarctic Ice Sheet collapse?, *Science*, *276*, 662–664, 1997.

Boucher, C., Z. Altamimi, and P. Sillard, The 1997 International Terrestrial Reference Frame (ITRF97), *IERS Tech. Note 27*, Obs. de Paris, Paris, 1999.

Bouin, M.-N., Traitement de données GPS en Antarctique: Mouvements crustaux, rebond post-glaciaire et systèmes de référence, Ph.D. thesis, Lab. de Géol. de l'Ecole Normale Supér. and Lab. de Rech. en Géod. de Ecole Nat. des Sci. Géogr., Paris, 1999.

DeMets, C., R. G. Gordon, D. Argus, and S. Stein, Current plate motions, *Geophys. J. Int.*, *101*, 425–478, 1990.

DeMets, C., R. G. Gordon, D. Argus, and S. Stein, Effect of recent revisions to the geomagnetic reversal timescale on estimates of current plate motions, *Geophys. Res. Lett.*, *21*, 2191–2194, 1994.

Denton, G. H., M. L. Prentice, and L. H. Burckle, Cainozoic history of the Antarctic ice-sheet, in *Geology of Antarctica*, edited by R. J. Tingey, pp. 365–433, Oxford Univ. Press, New York, 1991.

Dietrich, R., et al., GPS-derived crustal deformations in Antarctica (abstract), *Eos Trans. AGU*, *79, (45), Fall Meet. Suppl.*, F215, 1998.

Farrell, W. E., Deformation of the Earth by surface loads, *Rev. Geophys.*, *10*, 761–797, 1972.

Giovinetto, M., and C. Bentley, Surface balance in ice drainage systems of Antarctica, *Antarct. J. U. S.*, *20*, 6–13, 1985.

Herring, T. A., Global Kalmann Filter VLBI and GPS Analysis Program, Version 4.1, Mass. Inst. of Technol., Cambridge, 1998.

Huybrechts, P., Formation and disintegration of the Antarctic ice sheet, *Ann. Glaciol.*, *20*, 336–340, 1994.

Jacobs, S., H. Hellmer, C. Doake, A. Jenkins, and R. Frolich, Melting of ice shelves and the mass balance of Antarctica, *J. Glaciol.*, *38*, 375–386, 1992.

James, T., and E. Ivins, Predictions of crustal motions in Antarctica as deduced from the postglacial rebound and present-day ice mass variations, *J. Geophys. Res.*, *103*, 957–960, 1998.

Kamimuna, K., Crustal uplift around Syowa station, Antarctica, in *Geodesy on the Move, Int. Assoc. Geod. Symp.*, edited by Forsberg et al., Berlin, vol. 119, pp. 535–540, 1998.

King, R. W., and Y. Bock, Documentation for the MIT GPS analysis software: GAMIT, Mass. Inst. of Technol., Cambridge, 1993.

Larson, K. M., J. Freymueller, and S. Philipsen, Global plate velocities from the Global Positioning System, *J. Geophys. Res.*, *102*, 9961–9981, 1997.

McGuire, J. J., L. Zhao, and T. H. Jordan, GSDF inversion for higher moments of the stress glut rate tensor (abstract), *Eos Trans. AGU*, *79 (45), Fall Meet. Suppl.*, F458, 1998.

Nakada, M., and K. Lambeck, Late Pleistocene and Holocene sea-level change in the Australian region and mantle rheology, *Geophys. J.*, *96*, 497–517, 1989.

Nettles, M., T. C. Wallace, S. Beck, and G. Ekström, The March 25, 1998 Antarctic plate earthquake (abstract), *Eos Trans. AGU*, *79 (45), Fall Meet. Suppl.*, F462, 1998.

Okada, Y., Internal deformation due to shear and tensile faults in a half space, *Bull. Seismol. Soc. Am.*, *82*, 1018–1040, 1992.

Okal, E. A., Intraplate seismicity of Antarctica and tectonic implications, *Earth Planet. Sci. Lett.*, *52*, 397–409, 1981.

Pelayo, A. M., and D. A. Wiens, Seismotectonics and relative plate motions in the Scotia Sea region, *J. Geophys. Res.*, *94*, 7293–7320, 1989.

Peltier, W. R., Ice age paleotopography, *Science*, *265*, 195–201, 1994.

Rott, H., P. Skvarca, and T. Nagler, Rapid collapse of Northern Larsen ice shelf, Antarctica, *Science*, *271*, 788–792, 1996.

Saastamoinen, J., Atmospheric correction for the troposphere and the stratosphere in radio ranging of satellites, in *The Use of Artificial Satellites for Geodesy, Geophys. Monogr. Ser. vol. 15*, edited by S. W. Henriksen,

A. Mancini, and B. H. Chovitz, pp. 247–251, AGU, Washington, D. C., 1971.

Salbach, H., and W. Niemeier, Modeling of time-dependent deformation processes in the western Antarctic region from GPS epoch campaigns between 1995 and 1998 (abstract), *Eos Trans. AGU, 79 (45), Fall Meet. Suppl.*, F187, 1998.

Skvarca, P., Changes and surface features of the Larsen Ice Shelf, Antarctica, derived from LANDSAT and KOSMOS mosaics, *Ann. Glaciol.*, *20*, 6–12, 1994.

Smith, A. M., D. G. Vaughan, C. S. M. Doake, and A. C. Johnson, Surface lowering of the ice ramp at Rothera Point, Antarctic Peninsula, in response to regional climate change, *Ann. Glaciol.*, *27*, 113–118, 1998.

Toda, S., and R. S. Stein, Did stress triggering cause the large off-fault aftershocks of the March 25, 1998, m_w=8.1 Antarctic plate earthquake?, *Geophys. Res. Lett.*, *27*, 2301–2304, 2000.

Tushingham, A. M., and W. Peltier, ICE-3G: A new global model of late Pleistocene deglaciation based upon geophysical predictions of post-glacial relative sea-level change, *J. Geophys. Res.*, *96*, 4497–4523, 1991.

Verbitsky, M., and B. Saltzman, Behavior of the East Antarctic Ice Sheet as deduced from a coupled GCM/ice-sheet model, *Geophys. Res. Lett.*, *22*, 2913–2916, 1995.

Walpersdorf, A., L'observation de la tectonique active en Asie du Sud-Est par géodésie spatiale: Un projet GPS, Ph.D. thesis, Lab. de Géol. de l'Ecole Normale Supér., Paris, 1997.

M. N. Bouin, Laboratoire de Recherche en Géodésie, Ecole Nationale des Sciences Géographiques, Cité Descartes, 77455 Marne la Vallée Cedex 2, France. (bouin@ensg.ign.fr)

C. Vigny, Laboratoire de Géologie, Ecole Normale Supérieure, 24 rue Lhomond, 75231 Paris Cedex 05, France.

(Received January 24, 2000; revised June 15, 2000; accepted July 21, 2000.)